

DOI: 10.1515/amm-2016-0072

B. DYBOWSKI\*, T. RZYCHOŃ\*<sup>#</sup>, B. CHMIELA\*, A. GRYC\*

## THE MICROSTRUCTURE OF WE43 MMC REINFORCED WITH SiC PARTICLES

It is well known that the properties of a metal matrix composites depend upon the properties of the reinforcement phase, of the matrix and of the interface. A strong interface bonding without any degradation of the reinforcing phase is one of the prime objectives in the development of the metal matrix composites. Therefore, the objective of this work is to characterize the interface structure of WE43/SiC particles composite. Magnesium alloys containing yttrium and neodymium are known to have high specific strength, good creep and corrosion resistance up to 250°C. The addition of SiC ceramic particles strengthens the metal matrix composite resulting in better wear and creep resistance while maintaining good machinability. In the present study, WE43 magnesium matrix composite reinforced with SiC particulates was fabricated by stir casting. The SiC particles with 15 µm, 45 µm and 250 µm diameter were added to the WE43 alloy. The microstructure of the composite was investigated by optical microscopy, scanning electron microscopy, scanning transmission electron microscopy and XRD analysis. YSi and Y<sub>2</sub>Si reaction products are observed at the interfaces between SiC particles and WE43 matrix in the composite stirred at 780°C. Microstructure characterization of WE43 MMC with the 45 µm, stirred at 720°C showed relative uniform reinforcement distribution. Moreover, the Zr-rich particles at particle/matrix interface were visible instead of Y-Si phases. In the case of composite with 15 µm particles the numerous agglomerates and reaction products between SiC particles and alloying elements were observed. The presence of SiC particles assisted in improving hardness and decreasing the tensile strength and plastic properties.

*Keywords:* Metal Matrix Composite, WE43 matrix, SiC Reinforcement, Microstructure, Interface, Mechanical Properties

### 1. Introduction

Magnesium alloys are extensively investigated because of their low density (1.8g/cm<sup>3</sup>) and good mechanical properties. Magnesium alloys with aluminium additions (AZ- AM-types) are often used in automotive and aerospace industries, where the weight savings are essential. However, their further application is stopped by their low thermal stability (max. working temperature ≈120-150°C). Thus, magnesium alloys with rare earth (RE) elements were developed [1-4]. Addition of these elements leads to formation of Mg-RE phases, with much higher thermal stability than Mg<sub>17</sub>Al<sub>12</sub> phase, occurring in AZ and AM alloys [5,6]. Alloys with yttrium and neodymium (WE-type) additions may work up to 250°C. However, their main drawbacks are high price due to addition of expensive RE elements and many technological problems due to rapid oxidation of alloying elements [7].

Investigation revealed that further increase in creep resistance of magnesium based alloys may be increased by addition of ceramic particles, such as SiC. Ferkel et al. [8] revealed that pure magnesium reinforced with nanoscaled SiC particles exhibits creep resistance similar or even better than this, exhibited by a Mg-RE alloys. Many attempts were done to fabricate magnesium alloys based metal matrix composites (MMC) with SiC additions [9-11]. Majority of them, is however fabricated by means of milling and sintering. Cast composites are often processed

at room temperature for more homogenous distribution of the reinforcing phase. Stir casting seems to be promising method for the fabrication of Mg MMC reinforced with SiC. This method is economically effective and enables production of complex elements [10].

It is well known that properties of the composites depends upon properties of the reinforcing phase, matrix and interface between them [12]. Strong bonding between reinforcement and matrix enables transfer of the loads to the reinforcement. However, recent investigations conducted on the SiC reinforced WE54 alloy revealed, that in this case, load transfer by the particles does not contribute to the strengthening of the composite in a considerable degree. The main strengthening mechanisms revealed in this system are: strengthening by Hall-Petch relationship (increase of phase boundaries fraction), strengthening by Orowan mechanism and strengthening by differences in thermal expansion coefficients between reinforcement and matrix [13-14].

Available literature data show that SiC particles may act as heterogenous sites for crystallization of both α-Mg dendrites and eutectics in AZ91 alloy. However, it is true for submicron particles. In case of addition of larger ones, the grain size in the matrix increases. This leads to decrease of composites mechanical properties [15-16].

Many investigations were done on the interface reactions between magnesium alloys matrix and ceramic reinforcements. The model of SiC degradation in pure

\* SILESIA UNIVERSITY OF TECHNOLOGY, FACULTY OF MATERIAL SCIENCE AND METALLURGY, 40-019 KATOWICE, 8 KRASIŃSKIEGO STR., POLAND

<sup>#</sup> Corresponding author: tomasz.rzychon@polsl.pl

molten magnesium was proposed [17]. The degradation process proposed by this model begins with dissolution of  $\text{SiO}_2$  layer covering the SiC particles in liquid magnesium. This leads to formation of MgO and further dissolution of SiC particle. As the C solubility in the magnesium is low, graphite particles are precipitating. In the last stages,  $\text{Mg}_2\text{Si}$  phase and new,  $\beta$ -SiC phases are formed. The presence of alloying elements such as Al, Zn and RE leads to more complicated reactions. In the case of Mg-RE matrix alloys, products of interfaces reaction are mainly  $\text{RE}_3\text{Si}_2$  phases [18]. Zirconium oxide was also reported [19]. The following paper presents results of the investigations on fabrication of stir cast WE43 MMC reinforced with SiC particles. Particular attention was paid to matrix/reinforcement interface microstructure.

## 2. Research material and methodology

Material for the research was WE43 magnesium alloy metal matrix composite (MMC) reinforced with SiC particulates. The composite was produced by stir casting. Pure ingots of WE43 alloy were melted in resistance furnace under the protective atmosphere of 99.999% Ar. The melt was homogenized for about 20 min at 720°C and 780°C. The Mg-Y, Mg-Zr and Mg-Nd hardeners was added in order to compensate the chemical composition. Preheated (up to 300°C) SiC particulates (mean diameter 15  $\mu\text{m}$ , 45  $\mu\text{m}$  and 250  $\mu\text{m}$ ) were added after the ingots melting at the 720°C and 780°C. The stirring process was conducted for 15 minutes. The pouring process was conducted immediately after stirring into the graphite moulds, preheated to 200°C. The composites were poured at two different temperatures: 780°C and at 720°C. The pouring process as well as solidification of the composites were also conducted under protective atmosphere of Ar. The composites were cast in form of cylinders with diameter  $\varnothing=25\text{mm}$  and length  $l=300\text{mm}$ .

Microstructure of the composite was investigated by means of light microscopy (LM) on Olympus GX71 LM, scanning electron microscopy (SEM) on Hitachi S3400N and Hitachi S4200 SEM and scanning-transmission electron microscopy (STEM) on Hitachi HD-2300A. Chemical composition of the microstructure constituents was analyzed by energy dispersive spectroscopy (EDS) with detectors attached to SEM and STEM microscopes. The LM and SEM observations were conducted on both etched in 3% solution of  $\text{HNO}_3$  in ethyl alcohol and un-etched samples. Specimens for the STEM observations were prepared with FIB 2100 focused ion beam microscope.

Phase analysis were done by X-Ray diffraction (XRD) on JEOL JDX-7S diffractometer with a copper anode. Registration of XRD patterns was performed by 0.02° stepwise regression for  $2\theta$  ranging from 10° to 90°  $2\theta$ . Phase identification was performed using ICDD PDF-4+ database. Investigations were done both on solid specimens as well as on isolates prepared by dissolution of the composite in solution of 100ml of perchloric acid in 1000 ml of acetic acid.

Mechanical properties of each composite were investigated on Kappa 50DS tensile testing machine and Duramin A-300 hardness tester.

## 3. Research results

### 3.1. Composites matrix

Microstructure of the composites matrix consists of  $\alpha$ -Mg solid solution grains (Fig. 1a) and eutectic equilibrium  $\beta$  phase ( $\text{Mg}_3\text{RE}$  isomorphic to  $\text{Mg}_3\text{Gd}$ ) [5], distributed homogeneously within the interdendritic regions (Fig. 1b). The  $\alpha$ -Mg grains possess cellular morphology, however there are also observed grains with dendritic morphology. The solid solution in the vicinity of grain boundaries is enriched in the alloying elements – the concentration of Y solute atoms is up to 2.4% and Nd solute atoms up to 0.8%, while within the grains interior concentration of Y soluted atoms is only about 0.6%.

Moreover, non-metallic inclusions are observed in the composites matrix (Fig. 2a). They possess two morphologies, thread like – enriched in the yttrium as well as oxygen and fine particles – enriched in yttrium and oxygen (Fig. 2b) or yttrium, oxygen and zirconium (Fig. 2c).

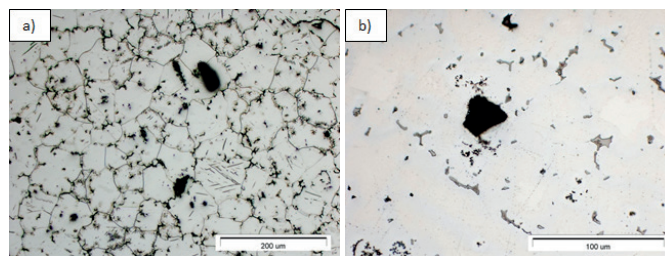


Fig. 1. Microstructure of the composites matrix, LM; a) grain structure of the WE43 alloy; b) eutectics morphology in the WE43 alloy

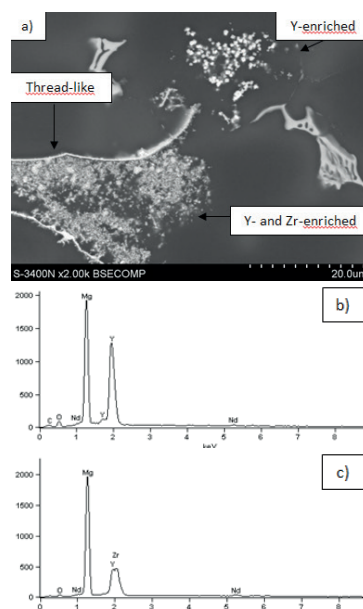


Fig. 2. Non-metallic inclusions in the composites matrix; a) Morphology of the inclusions, SEM; b) Results of EDS analysis of Y-enriched particles; c) Results of EDS analysis of Y- and Zr-enriched particles

### 3.2. Composites reinforcement

The SiC particles in each composite are distributed mainly at the grain boundaries and in the interdendritic regions. The reinforcement is distributed relatively homogeneously in the

composite reinforced with 15  $\mu\text{m}$  particulates, stirred at 780°C and in composite with 45  $\mu\text{m}$  particulates (Fig. 3a). In these cases, only single agglomerates are observed (Fig. 3b). The composite reinforced with 15  $\mu\text{m}$  particulates, stirred at 720°C exhibits non-uniform distribution of the particles. Majority of these particles is observed in form of numerous agglomerates (Fig. 3c).

The distribution of the 250  $\mu\text{m}$  particles on the transverse sections of the castings is relatively uniform (Fig. 3d). However, they tend to settle down in the crucible and in the mould, which leads to non-uniform distribution of the particles on the longitudinal sections.

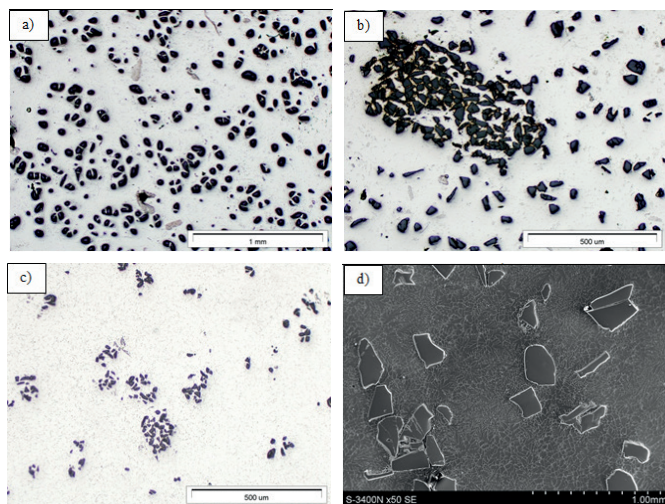


Fig. 3. Reinforcement distribution in different composites; a, b) 45  $\mu\text{m}$  particulates, LM; c) 15  $\mu\text{m}$  particulates, LM; d) 250  $\mu\text{m}$  particulates, SEM

### 3.3. Reinforcement/matrix interface

In each case, the interface between SiC particulates and WE43 alloy matrix is free from any voids. The matrix is well adhered to the particles, which is caused by good wettability of SiC with WE43 alloy. Products of reactions between the reinforcement and matrix are observed at the interfaces in each composite. It may suggest that matrix and particles are bonded chemically, not only physically.

In the composite cast at 780°C, numerous cuboidal precipitates are being observed between the WE43 matrix and SiC particulates (Fig. 4a). EDS investigations revealed that they are enriched in silicon as well as yttrium. The atomic ratio of Si to Y in these phases is close to 1. There are also observed phases with atomic ratio Si:Y is close to 0.5 (Tab. 1). In the vicinity of these phases some primary crystals of  $\text{Mg}_2\text{Si}$  phase were observed (Fig. 4b).

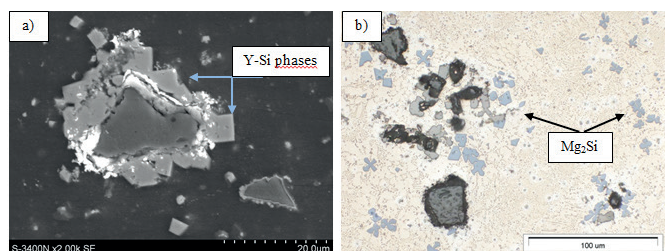


Fig. 4. Reaction products in the composite cast at 780°C; a) Y- and Si-enriched phases, SEM; b)  $\text{Mg}_2\text{Si}$  phases, LM

TABLE 1  
Chemical composition of the reaction products in composite cast at 780°C (at. %)

Phase:	Mg	Si	Y	Nd	Al
$\text{Mg}_2\text{Si}$	66.9	33.1	-	-	-
Cuboidal 1 (Si/Y $\approx$ 1)	22.0	38.9	36.9	2.2	-
Cuboidal 2 (Si/Y $\approx$ 0.5)	39.2	17.8	39.2	2.7	1.1

Composites cast at 720°C are characterized by considerable different interface structure. The interface between matrix and reinforcement is decorated by a thin layer (Fig. 5a), in which very fine particles are visible (Fig. 7). These particles are observed sometimes even 15  $\mu\text{m}$  from the reinforcement (arrow in the Fig. 5b). STEM observations revealed that the interface between particle and the matrix is strongly enriched in alloying elements – mainly in Zr and Y. These regions are also enriched in silicon. The Si content gradually decreases from the interface into the matrix, while zirconium content increases (Fig. 6). Apart from Si-Zr-Y layer at the interface (Fig. 5b), STEM observations revealed two more morphologies of phases occurring at and near the interface: cube-like precipitates, which contain mainly yttrium and oxygen (Fig. 7a, c); Second type – cuboids or spheres, which contain mainly Si and Zr (Fig. 7b, d). The ratio of Zr to Si in these phases is variable. The Zr/Si ratio vary from near 1 up to 3 and sometimes even higher (Tab. 2). This indicates that there are many types of Zr-Si phases formed at the interface. Impurities such as Fe or Al are often observed at the interfaces. Dy is also observed in phases present at the interface. Rare earth elements are always introduced into the melt in form of mixtures, not pure elements, so small amounts of elements such as Dy may be dissolved in the intermetallic phases. The peak for Cu on the EDS chart comes from the holder, at which specimen was introduced into the STEM chamber.

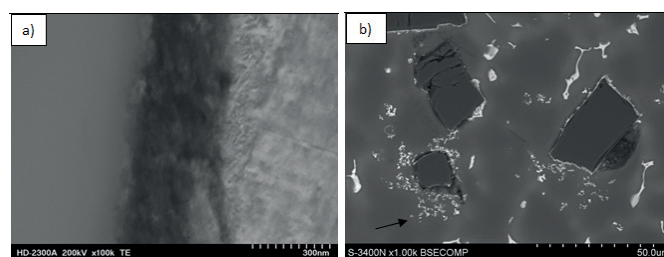


Fig. 5. Matrix/reinforcement interface structure; a) thin layer at the interface, STEM; b) layers of fine particles, SEM

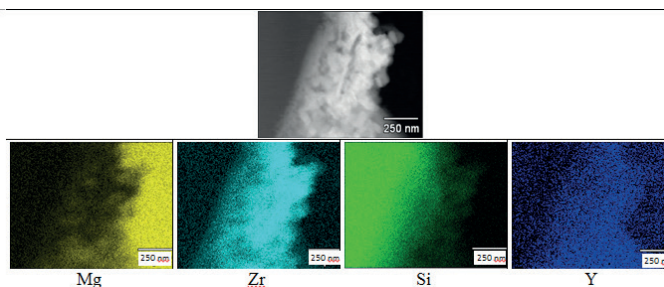


Fig. 6. Chemical composition of the SiC/WE43 interface

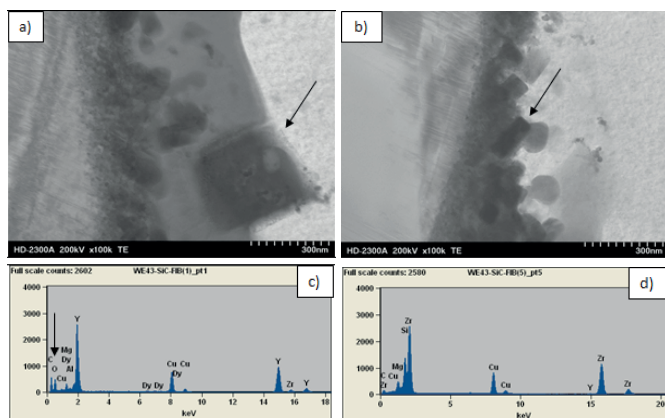


Fig. 7. Matrix/reinforcement interface structure STEM; a) Cubic phases; b) Cuboidal and spherical phases; c) EDS spectrum corresponding to the particle pointed in Fig. 7a; d) EDS spectrum corresponding to the particle pointed in Fig. 7b

TABLE 2

Chemical composition of different cuboidal phases at the SiC/WE43 interface in composite cast at 720°C (at. %)

Zr/Si ratio	Mg	Si	Zr	Al	Fe	RE
1.15	7.3	41.4	47.8	2.2	-	1.4
1.86	11.8	30.8	57.4	-	-	-
2.71	3.8	24.3	66.0	4.9	-	-
3.55	2.2	20.1	71.4	5.5	0.7	-
4.46	3.9	15.7	70.0	9.5	1.0	-

### 3.4. Phase analysis of the composites

The XRD phase analysis (Fig. 8) revealed that the microstructure of composite cast at 780°C consists mainly of  $\alpha$ -Mg solid solution. Moreover the diffractions lines of  $Mg_5Gd$  (ICDD 03-065-7133, cF448) phase were observed in the tested composite. This compound is isomorphous with the equilibrium  $\beta$  phase ( $a = 2.234$  nm). According to the literature and previous studies [5, 13, 20] the  $\beta$  phase has a  $Mg_{14}Nd_2Y$  composition in Mg-Y-Nd-Zr alloys and small differences in relative intensities between catalogue data for  $Mg_5Gd$  phase and experimental data were observed. and phase isomorphous to  $Mg_5Gd$ . The intermetallic phases observed at the  $\alpha$ -Mg solid solution grains (Fig. 1b) possess chemical composition similar to the  $Mg_{14}Nd_2Y$  compound (Tab. 3). The excess of Mg is probably caused by a large interaction volume and excitation of the  $\alpha$ -Mg matrix atoms. Presence of SiC particulates is also confirmed. Only YSi phase has been confirmed by the XRD investigations. Other phases were not confirmed, probably because of their low volume fraction in the composite.

Analysis of isolates received from composites cast at 720°C revealed presence of SiC particles and oxides such as:  $SiO_2$ ,  $Y_2O_3$ .  $Zr_2Si$  phase was also identified (Fig. 10). It should be noted that the identification of  $SiO_2$ ,  $Y_2O_3$ ,  $Zr_2Si$  compounds it is ambiguous due to their low content in the isolate and overlapping the diffraction lines. Other Zr-Si phases were not detected, probably because of their low volume fraction.

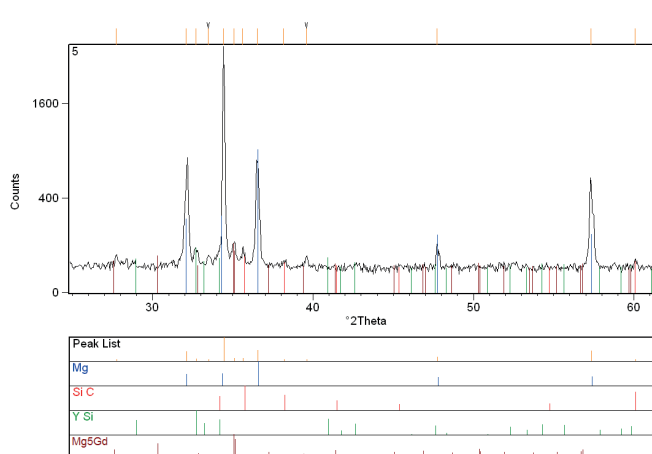


Fig. 8. XRD analysis results for SiC-WE43 composite cast from 780°C

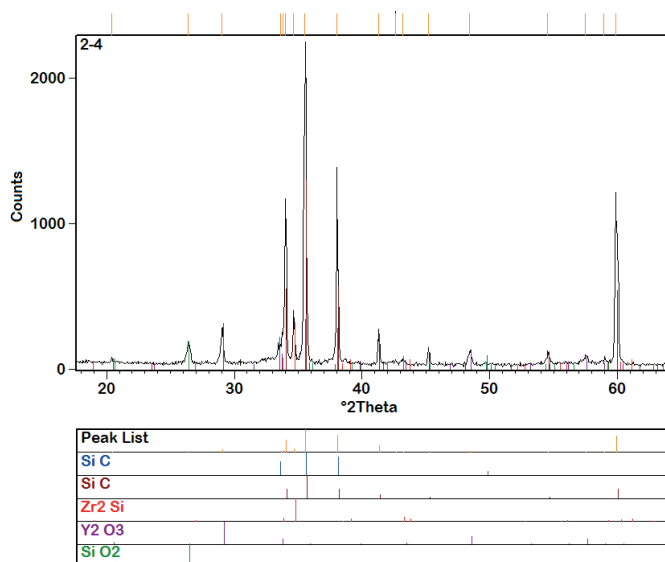


Fig. 9. XRD results for isolate from SiC-WE43 composite cast from 720°C

TABLE 3

Chemical composition of the phases isomorphous to  $Mg_5Gd$  (at. %)

Mg	Y	Nd
88.9	3.3	7.8

### 3.5. Mechanical properties of the WE43-SiC composites

Mechanical properties of each composite are shown in the Table 4. Addition of SiC particulates causes decrease of mechanical and ductile properties, when compared to the un-reinforced WE43 alloy. The addition of 15 $\mu$ m and 45 $\mu$ m particles causes similar decrease of the mechanical properties, while introduction of 250  $\mu$ m leads to further decrease of the plasticity and tensile strength of the composite. On the other hand, hardness of the composite is higher than this, exhibited by a pure WE43 alloy. It increases with increasing size of the particulates.

#### 4. Discussion

Presence of the non-metallic inclusions in the composites matrix is caused by oxygenating of liquid metal during the stirring process. Formation enthalpies of yttrium oxides and zirconium oxide at 720°C are more negative than formation enthalpy of magnesium oxide, therefore the yttrium and zirconium tend to react with oxygen before the magnesium and zirconium. As we did not find any MgO inclusions in the composite structure, it is possible that mainly Zr and Y are being oxygenated.

With increasing temperature, viscosity as well as density of the alloy decreases, so the movement of SiC particles is easier. This may lead to better homogeneity of the composite. However, at high temperature, SiC reinforcement react with the liquid alloy in a considerable way. Yttrium is the main element, reacting with SiC. It leads to the formation of massive YSi and probably Y<sub>2</sub>Si phases. Moreover, yttrium which reacts with reinforcement will not take a part in the further heat treatment of the composite, decreasing its final mechanical properties.

Stirring of the liquid alloy with SiC at 720°C may effect in inhomogeneous distribution of the particles in the matrix (mainly in case of particles with diameter close to 15µm). However, the particles react with the liquid alloy in much smaller degree. The proposed mechanism [17] of reactions in magnesium-SiC composite is following: thin SiO<sub>2</sub> layer, covering the SiC particles reacts with liquid magnesium, forming MgO. Elemental silicon formed in this reaction diffuses into the alloy, leading to formation of Mg<sub>2</sub>Si phase. In the second stage, liquid magnesium penetrates SiC particles. Carbon has a very low solubility in molten magnesium, which causes rapid precipitation of graphite. During cooling, new SiC crystals may be formed. This mechanism is true for pure magnesium matrix. These mechanisms are much more complicated in case of magnesium alloys, especially in case of magnesium alloys with rare earth elements. In available literature, products of reactions between SiC and Mg-RE alloys are noted to be mainly RE<sub>2</sub>Si<sub>3</sub> phases. Our investigations on composite stirred at 780°C confirmed, that in case of alloys containing rare earth elements, yttrium reacts preferentially with particles. However, in the available literature, there is no information about formation of Zr-Si type phases. Based on the conducted investigations, following mechanism for WE43 – SiC composite cast at 720°C is proposed: thin SiO<sub>2</sub> layer is penetrated with liquid alloy. As the yttrium is more reactive than magnesium (Formation enthalpy of Y<sub>2</sub>O<sub>3</sub> at 720°C is equal about -518 KJ/mol, while of MgO -128.5 KJ/mol)

its oxides are being formed. Remaining silicon reacts with zirconium, forming the Zr-Si phases. In the present work, Zr<sub>2</sub>Si phase was identified. However, EDS analysis showed, that the chemical composition of Zr-rich particles deviated from the stoichiometric Zr<sub>2</sub>Si composition, thus other Zr<sub>x</sub>Si<sub>y</sub> phases may be also formed. As there are no evidences of any carbides at the interface, it may be concluded, that Zr-Si layer acts as an effective blocker of diffusion processes, preventing the further decomposition of SiC particles.

The structure of the composite cast at temperature of 720°C, reinforced with 45µm particles is relatively homogenous, with thin reaction layers at the reinforcement/matrix interface. Moreover, yttrium does not take a considerable role in the reactions with the particles. Yttrium remaining within the matrix enables further heat treatment of the composite, leading to increase of the mechanical properties.

Mechanical properties of the fabricated composite are not satisfying. Cabbibo et al. [13] revealed that in magnesium alloy-SiC composites main strengthening mechanisms are strengthening due to Hall Petch relationship (increase of phase boundaries), strengthening by Orowan mechanism and strengthening by different thermal expansion coefficients between the matrix and reinforcement. As the introduced particles have a large size, first two mechanisms do not play an important role. Also third one mechanism, is not activated in ambient temperature. Moreover, large particles may act as a structural notches, decreasing the mechanical properties. Creep resistance however may be improved, due to activation of thermal expansion coefficients strengthening.

#### 5. Conclusions

WE43 alloy matrix composite reinforced with SiC particulates was successfully produced via stir casting. The best result was achieved for the composite stirred at 720°C, reinforced with 45µm SiC particulates.

Stirring at 780°C causes reactions between matrix and reinforcement, leading to formation of massive YSi and Y<sub>2</sub>Si phases at the matrix/particle interface decreasing plastic properties of the composite.

Stirring at 720°C ensures less homogenous distribution of reinforcement, however, reactions at the interfaces leads to formation of thin layers of Zr-Si phases.

Addition of SiC particles with diameters varying from 15µm to 250µm leads to decrease of mechanical and plastic properties of the material and increase of its hardness.

TABLE 4

Mechanical properties of the WE43-SiC composites

Material	Particle diameter [µm]	Stirring temperature [°C]	Stirring time [min]	Hardness HV2	R <sub>m</sub> [MPa]	R <sub>0.2</sub> [MPa]	A <sub>5</sub> [%]
WE43	-	-	-	59±4	166±18	113±9	6.7±1.5
WE43 + 10% SiC	15	720	15	68±5	142±4	103±6	2.9±0.3
WE43 + 10% SiC	15	780	15	66±7	146±9	111±12	2.8±0.2
WE43 + 10% SiC	45	720	15	71±6	149±16	125±14	3.0±0.1
WE43 + 10% SiC	250	720	15	81±4	112±11	89±6	1.1±0.1

### Acknowledgments

The present work was supported by the National Centre for Research and Development under the project LIDER/29/198/L-3/11/NCBR/2012

### REFERENCES

- [1] H. Friedrich, B.L. Mordike, *Magnesium Technology, Metallurgy, Design Data, Applications*, Springer-Verlag Berlin Heidelberg 2006.
- [2] A.A. Luo, *Int. Mater. Reviews* **49** (1), 13 (2003).
- [3] B. Płonka, K. Remsak, M. Nowak, M. Lech-Grega, P. Korczak, A. Najder, *Arch. Metall. Mater.* **59**, 377 (2014).
- [4] K. Maruyama, M. Suzuki, H. Sato, *Metall. Mater. Trans. A.* **33**, 875 (2002).
- [5] A. Kielbus, T. Rzychoń, *Mater. Sci. Forum* **690**, 214 (2011).
- [6] T. Rzychoń, A. Kielbus, L. Lityńska-Dobrzyńska, *Mater. Charact.* **83**, 21 (2013).
- [7] B. Dybowski, A. Kielbus, R. Jarosz, *Arch. Metall. Mater.* **59**, 245 (2014).
- [8] H. Ferkel, B.L. Mordike, *Mater. Sci. Eng. A* **298**, 193 (2001).
- [9] M.J. Shen, X.J. Wang, M.F. Zhang, X.S. Hu, M.Y. Zheng, K. Wu, *Mater. Sci. Eng. A* **601** 58 (2014).
- [10] X.J. Wang, N.Z. Wang, L.Y. Wang, X.S. Hu, K. Wu, Y.Q. Wang, Y.D. Huang, *Mater. Des.* **57**, 638 (2014).
- [11] L. Lu, C.Y.H. Lim, W.M. Yeong, *Compos. Struct.* **66**, 41 (2004).
- [12] G. Inem, B. Pollard, *J. Mater. Sci.* **28**, 4427 (1993).
- [13] M. Cabibbo, S. Spigarelli, *Mater. Charact.* **62**, 10, 959 (2011).
- [14] Z. Száráz, Z. Trojanová, M. Cabbibo, E. Evangelista, *Mater. Sci. Eng. A* **462**, 225 (2007).
- [15] S. Zhou, K. Deng, J. Li, S. Shang, W. Liang, J. Fan, *Mater. Des.* **63**, 672 (2014).
- [16] Y. Cai, D. Taplin, M.J. Tan, W. Zhou, *Scr. Mater.* **41**, 967 (1999).
- [17] T. Epicier, F. Bosselet, J.C. Viala, *Interface Sci.* **1**, 213 (1994).
- [18] K.N. Braszczyńska, L. Lityńska, A. Zyska, W. Baliga, *Mater. Chem. Phys.* **81**, 326 (2003).
- [19] W. Yang, G.C. Weatherly, D.W. McComb, D.J. Lloyd, *J. Microsc.* **185**, 292 (1997).
- [20] T. Rzychoń, J. Szala, and A. Kielbus, *Arch. Metall. Mater.* **57**, 245 (2012).

*Received: 10 March 2015.*